EFDA–JET–CP(10)05/23

U. Kruezi, M. Lehnen, V. Philipps, S. Brezinsek, G. Sergienko,
S. Bozenkhov, S. Jachmich, P.D. Morgan, G.F. Matthews
and JET EFDA contributors

Massive Gas Injections in JET - Impact on Wall Conditions

Massive Gas Injections in JET - Impact on Wall Conditions

U. Kruezi, M. Lehnen, V. Philipps, S. Brezinsek, G. Sergienko,
S. Bozenkhov, S. Jachmich, P.D. Morgan, G.F. Matthews
and JET EFDA contributors*

JET-EFDA, Culham Science Centre, OX14 3DB, Abingdon, UK

[1]IEF - Plasmaphysik, FZJ Jülich GmbH, Association EURATOM-FZJ, D-52425 Jülich, Germany
[2]Max-Planck-Institut für Plasmaphysik, Assoziation EURATOM-IPP, 17491 Greifswald, Germany
[3]LPP - LVP, Association EURATOM-Belgian State, ERM/KMS, B-1000 Brussels, Belgium
[4]EURATOM/CCFE Fusion Association, Culham Science Centre, Abingdon, OX14 3DB, UK
** See annex of F. Romanelli et al, “Overview of JET Results”,*
(Proc. 22 nd IAEA Fusion Energy Conference, Geneva, Switzerland (2008)).

Preprint of Paper to be submitted for publication in Proceedings of the
19th International Conference on Plasma Surface Interactions, San Diego, California, USA.
(24th May 2010 - 28th May 2010)

ABSTRACT

Disruptions are a critical issue for large scale tokamak due to a risk of damage to the plasma facing components. Massive Gas Injection (MGI) is considered as a 'last resort' method for disruption mitigation. A MGI system based on the disruption mitigation valve has been brought into operation at JET. Injections of neon in the range of 0.16-0.9kPa·m^3, argon (0.12-0.86kPa·m^3) and its mixtures with deuterium (0.24-1.28kPa·m^3) show distinct effects on the machine condition during and after MGI-induced disruptions. This contribution focuses, using mass and VUV spectroscopy, on the impact of MGI on the wall conditions.

1. INTRODUCTION

Disruptions, the fast accidental losses of the plasma current and stored energy in tokamaks, are a critical issue for reactor-scale fusion facilities like ITER. They present a serious risk of severe damage to the Plasma Facing Components (PFCs). The avoidance of damage is essential for the upcoming ITER-Like Wall (ILW) experiments in which beryllium and tungsten will be used as plasma-facing materials in the main chamber and divertor at JET, the tokamak experiment closest to ITER in terms of operating parameters and size.

Massive Gas Injection (MGI) is considered as a "last resort" method for disruption mitigation. The injection of noble gases is preferred because of their high recycling and low sticking probabilities to the wall, which should enable a reliable plasma breakdown and normal plasma operation after gas injection. To allow scaling of the mitigation efficiency towards ITER and to study the possibility of a JET protection by MGI a Disruption Mitigation Valve (DMV) has recently been brought into operation JET.

The application of MGI ($10\%Ar/90\%D_2$ mixtures) into a disruptive plasma results in a conversion of about 50% of the thermal energy into radiation. Thus a reduction of the heat loads to the PFCs can be expected [Arnoux, Huber]. During deliberately-induced Vertical Displacement Event disruptions (VDE), MGI diminished halo currents by up to a factor of 2.5 while the vertical mechanical forces were reduced by 30% [LehnenNew]. Furthermore, the DMV presents a useful tool to create and study, or to suppress, Runaway Electrons (REs). While MGI of pure Ar could be used to create REs, injections of gas mixtures with D_2 reliably suppress their generation. The latter is based on a higher fuelling efficiency of the gas mixtures. Beside these mitigation effects, MGI can lead to a deconditioning of the first wall with consequences for the subsequent discharges. On the other hand, deliberate disruptions have been proposed as a method for tritium release [Whyte].

This contribution focuses, using mass and VUV spectroscopy methods, on the impact of MGI on wall conditions and consequences for the subsequent machine operation.

2. THE DISRUPTION MITIGATION VALVE AT JET

The JET set-up of the Disruption Mitigation Valve (DMV) and the function principle have been presented in [KrueziEps]. It is mounted on one of the the probe drives on top of the JET octant 1 and is connected via a 4m long tube (diameter 40 mm, distance to separatrix ~0.5m) to the JET vacuum vessel. This high pressure valve (injection pressure 0.2-3.6MPa, valve orifice 10mm, injection volume $6.5\times10^{-4}m^3$) consists exclusively of non-ferro-magnetic materials and therefore stays operational inside high magnetic fields as present in fusion devices. The maximum injected amount of gas is achieved at the maximum allowed pressure of 3.6 MPa and is equal to 0.85 – $1.0kPa\cdot m^3$ ($1.9 – 2.3\times10^{23}$ particles) depending on the gas type, with the amount being higher for lighter gases. The gases which can be used for MGI at JET are Ar, Ne, He, H_2/D_2 and mixtures of these which can be created inside the injection volume with an accuracy of 1%. The quantity of injected helium is restricted to $0.3\ kPa\cdot m^3$ in JET due to the cryogenic divertor pump; the low pumping speed and high heat conductance can lead to a spontaneous regeneration of the cryogenic panels. More technical details and characterisation of the valve can be found in [Kruezi,DMVx3].

3. CONSEQUENCES OF MASSIVE GAS INJECTION EXPERIMENTS ON MACHINE CONDITION

Standard disruption mitigation by MGI must not only ensure a reduction in loads, but also must maintain the machine conditions needed for reliable operation. It should be noted that during the open loop MGI experiments an incomparably higher quantity of gas is injected in total (over many discharges) to provoke and study consecutive disruptions. These amounts would be smaller if the DMV would be used as a closed loop machine protection system to mitigate “natural” disruption which appearance should be reduced in first place.

3.1 GAS RELEASE AFTER MGI DISRUPTIONS

Disruptions in general lead to an enhanced particle release from the wall, of the order of 10^{22} at JET (e.g. 1.8×10^{22} for the VDE disruption in JET pulse 79554). This release depends on the total energy in the plasma, consisting of the thermal energy and the magnetic energy. They are converted during the disruption into radiation, possible electron runaway current and convective heat loads to the PFCs. As a consequence their temperature increases [Arnoux], followed by particle release, either via thermal, chemical or particle-induced desorption from the wall [Winter]. The latter plays a major role for injected noble gases. To deduce the number of particles released from the wall the pressure decay after the disruption can be observed and the amount of gas can be calculated using the ideal gas law equation. However, in the case of MGI mitigated disruptions it is hardly possible to specify these quantities absolutely for JET. Two reasons can be mentioned for this. First, the amount of injected gas is one order of magnitude higher than the expected number of particles which are released and they are therefore difficult to distinguish. Second, for vacuum pressure measurements at JET, Penning gauges are used which operate reliably only in high vacuum. Thus they are saturated during MGI (pressure rises typically above 0.1Pa), and are sensitive to the gas composition, which obviously is modified during and shortly after the MGI.

However, MGI with D_2 mixtures have shown a distinct effect for the first consecutive pulse.

For larger MGI injections with more than 0.26kPa·m^3 of D_2 in the gas mixtures a Non-Sustained plasma Breakdown (NSB) has been observed at the beginning of the consecutive pulse. The reason is a strong gas release during the plasma start-up phase due to a large amount of retained D_2 in the wall. The released gas rate is of the order 1.6×10^{21} particles/s which causes a release of typically 3.5-5.0Pa·m^3 depending on the duration of the NSB. This additional gas, which cannot be compensated by lower gas pre-filling, typically in the range of 1 Pa·m^3 at JET, prevents the normal plasma breakdown and therefore has to be accepted as a usual consequence of MGI D_2 mixtures. A normal plasma breakdown has been observed in the pulse following the NSB with gradually stronger but acceptable outgasing of deuterium during the pulse.

In general outgasing occurs on a short time scale in an exponential manner defined by the pumping efficiency of the pump system and on a longer time scale. The latter approaches a decay proportional to $\sim (t\text{-}t_{\text{disruption}})^{-a}$ which has been measured with the help of a quadrupole mass spectrometer. A typical behaviour for different gas species is shown in figure 2.

The exponent a is the range of a = 0.34…1.09 and varies between the injected gases and depends also on the injected quantity as listed in Table 1. A quantitative analysis is very difficult because of the unavailable calibration of the shown signals. A longer observation of the signals would be preferable to observe any change in the outgasing rate but is also not available for this diagnostic.

However, the relative behaviour indicates a stronger outgasing for argon after MGIs in the first 1000 seconds. Argon in gas mixtures with deuterium differs from this behaviour. In general the outgasing reduces the concentration of impurities after an MGI terminated pulse but is expected to be on much longer time scales then the time between two plasma pulses (e.g. 20 min at JET). The remaining gas in the wall may therefore influence consecutive plasma pulses, where noble gas atoms and deuterium molecules could be released and may enter the plasma.

3.1 CONSEQUENCES FOR CONSECUTIVE PLASMA PULSES AFTER MGI

The MGI experiments at JET during the campaigns in 2008/2009 have been performed with various gases and under various plasma conditions (plasma current and magnetic field, L-mode, H-mode etc.). The plasma pulses terminated by MGI were designed in order to be able to study the consequences of a prior MGI disruption: During the limiter phase the plasma contact with the PFCs has been varied vertically and horizontally at the low and high field side as shown in figure 2 (left). This could be used to determine gradually the source of the impurity outgasing. In the following divertor phase (Fig.2 right) strike point sweeps have been applied.

The result of these plasma sweeps can be seen during a plasma pulse after a MGI with *Ar* in the VUV ArXVI (35.392nm) signal shown for JET pulse number #77813 in figure 3.

The modulation of the signal before the divertor phase (dashed line) is a result of the wall clearance at the low and high field sides. The strike points sweeps (between dotted lines) during the divertor phase are responsible for an exponential decay of the MGI impurity as indicated in figure 2. The decay times are about several seconds (τ = 2.8-5.2s) and increase with each additional MGI terminated plasma pulse. The decay times for neon stay constant at a level of about $\tau = 3.4$s. This strike point sweeping phase is followed by a phase with the strike point located in the corner of the divertor, where efficient pumping with the divertor cryogenic pump in JET occurs. Either this phase was followed by a H-mode or the plasma pulse was kept in L-mode with only ohmic heating before the MGI termination of the pulse.

In figure 4, MGI injections of different N*e* quantities (Fig.4a) are shown together with the resulting average spectroscopic VUV *NeVIII* (77.041nm) signal normalised to the line averaged electron density (fig.b) during limiter (plasma contacts with inner and outer limiter are shown seperately), which is proportional to the *Ne* concentration in the plasma. Additionally, a smaller amount has been injected with the help of the JET fuelling system (green bar) and one pulse was terminated by a low-q disruption (grey bar). As it can be seen, the signal varies gradually with the amount of injected gas. Contamination of the wall with *Ne* or other noble gases might depend on the condition prior to the injection, therefore a parametric graph (the integral spectroscopic signal versus the integral amount of injected gas) has been created using data of Fig.4(a,b). This graph (shown in Fig.5) takes into account the history effect.

Additional signals for pure *Ar* and Ar/D_2 mixture injections were added to figure 5. In the neon case one can see that neon release grows up nonlinearly for small gas injections and is proportional to the injected amounts for large injections.

This is an indication that the *Ne* gas quantities used for MGI are sufficient to saturate the wall. Smaller quantities of gas gain a larger fraction of kinetic energy per particle during the disruption and the associated energy conversion and therefore gas can penetrate deeper into the PFCs and the wall. This can be seen as a reason for the slower outgasing for smaller injected gas quantities presented in Table 1. The repetition of the injection sequence shows an identical behaviour after a low-q “disruptive” cleaning, which reduced the neon concentration back to the initial background level.

Argon shows a different behaviour. Each MGI injection causes a nonlinear increase of the argon concentration in the next plasma pulse. No saturation can be observed for *Ar*. The highest concentrations in contrast to *Ne* can be observed during the divertor phase. A low-q disruption reduces the concentration and a further injected amount leads to a similar behaviour seen before the low-q disruption. Such accumulation behaviour is caused by trapped argon atoms in the carbon PFCs, which reaches saturation at about 2×10^{19} atoms m^{-2} with impact energies above 250eV and are almost fully released upon hydrogen ion bombardments with the same energy [Winter]. This explains why a strong particle release can be seen during the divertor phase, as the divertor itself represents the largest carbon area in JET.

The trapped argon can easily be removed by deuterium ions and this explains why argon in mixtures with deuterium does not show a strong tendency to accumulate, moreover reduces the argon concentration as a result of previous pure argon injections.

As an additional consequence MGI influences on the outgasing rate of deuterium. This can be seen in figure 4c, which is according equation 1 a signal proportional to the average outgasing rate.

$$\frac{dN}{dt} = \frac{N}{\tau_P} + \Gamma_{Fuel} + \Gamma_{Outgas} \Rightarrow$$

$$\int \Gamma_{Outgas}\, dt \propto \left(N(t) + \int \frac{N}{\tau_P}\, dt \right) \int \Gamma_{Fuel}\, dt$$

N is the total particle number in the plasma, τ_P the particle confinement time which can be assumed as constant, Γ_{Fuel} the gas fuelling rate given by the fuelling feedback control signal and Γ_{outgas} the outgasing rate.

Strong outgasing appears after the first *Ne* injection and decreases with the consecutive injections. This is confirmed by mass spectrometer data of D_2^+ (m/e=4)and CD_3^+ (m/e=18) which is an indication of a reduction of deposited layers. Disruptions without MGI show the opposite effect, where the wall is loaded with deuterium and layers appear again. Hence, MGI provoked disruption might be useful method for tritium retention. Further analysis is needed.

CONCLUSIONS

A MGI system has been brought into operation at JET and recent experiments with various injected gas species (neon, argon mixtures of these with deuterium) have shown mitigation effects such as reduction of halo currents and mechanical forces during VDEs.

However, the injection of impurities can influence the machine condition for the plasma pulses after the MGI. MGIs with neon show a saturation effect and *Ne* retention even at low injected quantities. The outgasing rate of neon after a MGI is higher in comparison with normal plasma pulses and low-q disruptions. One low-q disruption reduced the neon concentration down to the background level.

MGI with pure argon shows a strong accumulation in consecutive pulses building up high a concentration due to trapped argon in carbon PFCs.

Injected mixtures with deuterium have proven to be very efficient to suppress runaway electrons and to mitigate the deteriorating effects on PFCs and structural components caused by disruptions. However, as a consequence the consecutive plasma pulse will suffer from the strong outgasing of 3.5-5.0×Pa·m^3 in the plasma start-up which will cause a NSB. This particle release is sufficiently high to permit normal operation afterwards.

ACKNOWLEDGEMENT

This work, supported by the European Communities under the contract of Association between EURATOM/FZJ, was carried out within the framework of the European Fusion Development Agreement. The views and opinions expressed herein do not necessarily reflect those of the European Commission.

REFERENCES

[1]. U. Kruezi et al., EPS09, Sofia

[2]. A. Savchkov, K.-H. Finken, G. Mank, Review Scientific Instruments. **73** 3490 (2002)

[3]. S. A. Bozhenkov, K.-H. Finken, M. Lehnen, Review Scientific Instruments **78** 033503 (2007)

[4]. K.-H. Finken, M. Lehnen, S. A. Bozhenkov, Nuclear Fusion **48** (2008) 115001

[5]. G. Arnoux et al, at this conference

[6]. A. Huber et al., at this conference

[7]. M. Lehnen et al. to be published

[8]. D.G. Whyte & J.W. Davis, J. Nuclear Material **337-339** (2005) 560

[9]. J. Winter, Plasma Physics Controlled Fusion **38** (1996)

MGI quantity	Ar	Ne	10%Ar/ 90%D_2
0.43×10^{23}	0.87[1]… 1.04	-	0.62… 0.71
1.15×10^{23}	-	0.80	-
2.25×10^{23}	1.05... 1.09	0.85	0.55[2]… 0.78
NSB	-	-	0.28… 0.34
0.025×10^{23}	0.45 (Ne)		
Reference plasma pulse	0.52		
low-q disruption	0.47…0.55		

Table 1: Exponent a for $(t-t_{disruption})^{-a}$ *for various gases and conditions.*
[1] *first pulse after disruption.* [2] *two pulses after 4 pure Ar injections*

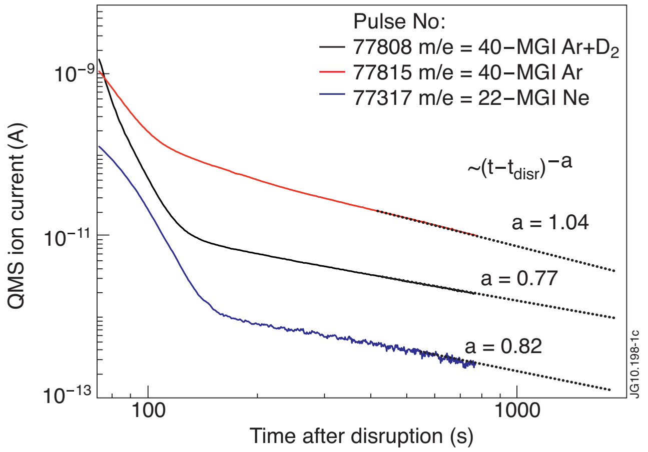

Figure 1: Gas release measured with quadrupole mass spectrometry after MGI provoked disruptions with Ne (m/e=22), Ar (m/e=40) and 10%Ar/90%D_2 *(m/e= 40 Ar) at* $t_{disrupt}$ *showing a time dependence* $\sim(t-t_{disrupt})^{-a}$

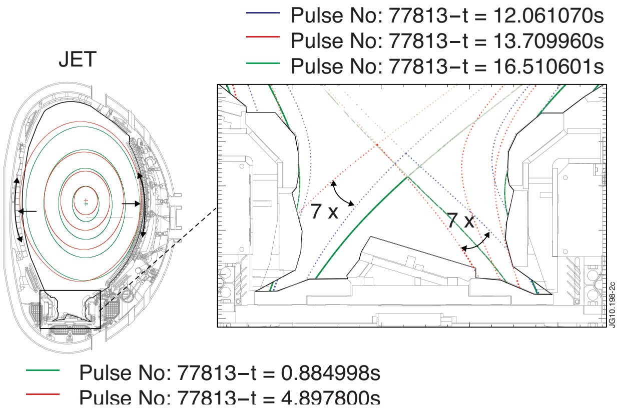

Figure 2: Magnetic configuration representative for the plasma experiments during limiter phase with plasma sweeps at high and low field side. (right) Indicated strike point sweeps during the divertor phase.

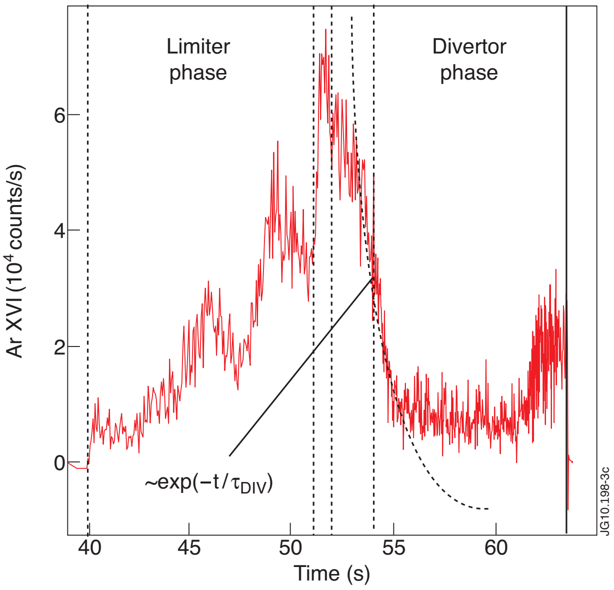

Figure 3: Temporal behavior of the relative argon concentration during a plasma pulse. Divertor sweeping phase is applied between the doted lines. The exponential decay during this phase is indicated.

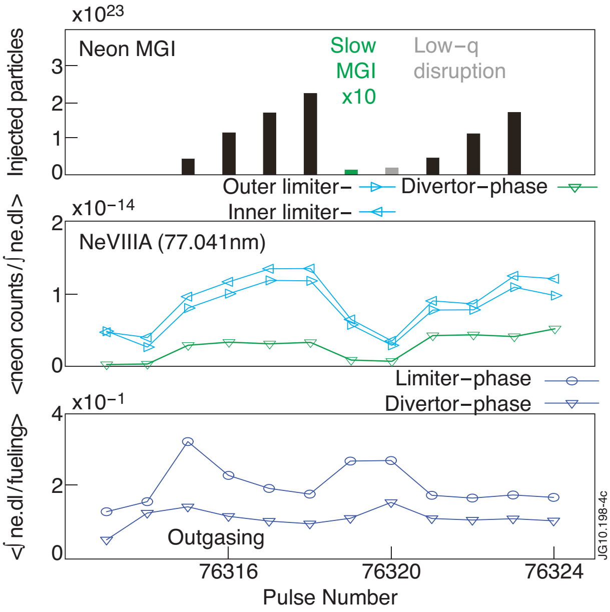

Figure 4: (a) Influence of neon MGI on the (b) average concentration (spectroscopic) of the injected Impurities in the consecutive plasma pulse during outer-inner limiter and divertor phase Ne Pulse No: 76313-76324, $B_t = 1.8\text{-}3.0$ T, $I_P = 2.0$MA, ohmic and (c) the outgasing rate.

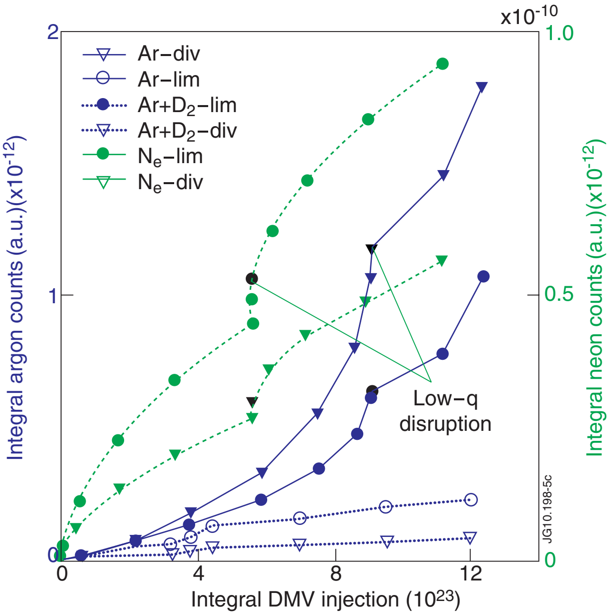

Figure 5: Concentration of MGI Impurities in consecutive plasma pulses parametric graph of MGI with various gases (including Ne Pulse No: 76313-76324 fig.2).